https://doi.org/10.5194/egusphere-2026-3311
Preprint. Discussion started: 30 June 2026

Indicator-dependent vegetation trends and interannual variability across Asia–Oceania from NDVI, vegetation optical depth, and model-based GPP during 2000–2021

Madoka Koshino[1, 2], Kazuhito Ichii[1, 2], Misaki Hase[1, 2], Daniel Henri[1], Beak Munseon[1, 2]

[1] Center for Environmental Remote Sensing (CEReS), Chiba University, Chiba, 263-8522, Japan
[2] Graduate School of Science and Engineering, Chiba University, Chiba, 263-8522, Japan

Correspondence to: Madoka Koshino (koshino.m.1212@chiba-u.jp) and Kazuhito Ichii (ichii@chiba-u.jp)

Abstract. Vegetation change has been widely monitored using satellite-derived vegetation indices, particularly the Normalized Difference Vegetation Index (NDVI). However, different vegetation indicators represent different aspects of ecosystem conditions and may provide contrasting views of long-term vegetation change. In this study, we compared long-term trends and interannual variability among multiple indicators including two NDVI datasets, Vegetation Optical Depth (VOD), and gross primary production (GPP) simulated by a process-based ecosystem model VISIT across the Asia–Oceania region during 2000–2021. Long-term trends were estimated using Sen's slope, and interannual variability was evaluated using detrended and standardized annual anomalies. Both NDVI datasets showed widespread positive trends across East Asia and northern Eurasia, whereas VOD exhibited weaker and more spatially heterogeneous trends, particularly in high-latitude regions. East Asia showed relatively consistent positive trends among NDVI, VOD, and GPP, suggesting coherent increases in vegetation greenness, biomass, and ecosystem productivity. In contrast, substantial discrepancies were observed in Siberia, where strong NDVI greening was not consistently accompanied by increases in VOD or GPP. Comparisons of interannual variability also revealed regional differences in agreement among indicators, with stronger relationships among NDVI, VOD, and GPP in East Asia and some semi-arid regions than in boreal ecosystems. These results indicate that assessments of vegetation change depend strongly on the indicator used and that different indicators capture different aspects of ecosystem dynamics. Combining optical, microwave, and model-based indicators therefore provides a more complete understanding of vegetation change across the diverse environments of Asia–Oceania.

1 Introduction

Terrestrial ecosystems play a central role in regulating the global carbon cycle and climate system, making long-term monitoring of vegetation dynamics essential for understanding ecosystem responses to climate change and human activities (Friedlingstein et al., 2022). Vegetation influences exchanges of carbon, water, and energy between the land surface and atmosphere, and changes in vegetation activity can strongly affect climate–carbon feedbacks. Satellite remote sensing provides a unique opportunity to monitor vegetation continuously over large spatial and temporal scales. In recent decades, satellite

https://doi.org/10.5194/egusphere-2026-3311
Preprint. Discussion started: 30 June 2026

observations have revealed widespread vegetation changes, including large-scale greening trends across many regions of the world (Zhu et al., 2016; Chen et al., 2019; Piao et al., 2020; Forkel et al., 2016). Such long-term observations have therefore become increasingly important for evaluating terrestrial ecosystem change and its implications for the Earth system.

Although NDVI has been the most widely used satellite-based indicator for long-term vegetation monitoring, sole reliance on this index presents significant limitations that can lead to incomplete or misleading assessments of vegetation dynamics. Long-term NDVI datasets derived from sensors such as AVHRR and MODIS have been extensively used to evaluate vegetation greening and browning trends from regional to global scales (Zhu et al., 2016; Chen et al., 2019). Many studies have reported substantial vegetation increases in Asia and other regions and attributed these trends to factors such as CO_2 fertilization, climate variability, and land-use management. However, NDVI primarily reflects canopy greenness and optical properties and may not adequately represent other aspects of ecosystem change. NDVI is affected by atmospheric conditions, cloud contamination, sensor characteristics, and saturation in densely vegetated regions (Myneni et al., 1995). Furthermore, recent studies have indicated that changes in interannual variability (IAV) of vegetation greenness derived from different satellite products can be inconsistent or even conflicting across large portions of the global vegetated surface, particularly in tropical regions (Tian et al., 2024). Consequently, assessments based solely on NDVI may provide incomplete or potentially misleading interpretations of vegetation dynamics, particularly in ecosystems with complex vegetation structure or strong hydroclimatic variability.

Different vegetation indicators capture different aspects of ecosystem structure and function, providing complementary perspectives on terrestrial ecosystem dynamics. To complement optical vegetation indices, Vegetation Optical Depth (VOD), derived from passive microwave observations, has increasingly been used to monitor vegetation dynamics. VOD is sensitive to vegetation water content and aboveground biomass and is less affected by cloud cover and atmospheric conditions than optical indices (Frappart et al., 2020; Konings et al., 2019; Zotta et al., 2024). Previous studies have demonstrated the usefulness of VOD for detecting drought stress, biomass variability, and ecosystem responses to climate fluctuations in diverse environments including drylands (Tian et al., 2016; Momen et al., 2017; Rao et al., 2019). In addition, gross primary production (GPP) derived from process-based ecosystem models represents the functional aspect of vegetation activity through carbon uptake. Unlike optical or microwave indicators, model-derived GPP integrates environmental controls such as temperature, precipitation, radiation, and atmospheric CO_2 concentration. Because NDVI, VOD, and GPP represent different aspects of vegetation structure, water status, and ecosystem function, respectively, they may exhibit substantially different long-term trends and interannual variability even within the same region. Comparing these indicators is therefore meaningful for clarifying which aspect of vegetation dynamics each captures and for understanding the extent to which structural, hydrological, and functional changes in vegetation are coherent or divergent.

Systematic evaluations of consistency and disagreement among optical, microwave, and model-based vegetation indicators remain limited despite their increasing availability. Most previous studies have focused on single indicators or comparisons

https://doi.org/10.5194/egusphere-2026-3311
Preprint. Discussion started: 30 June 2026

among similar datasets, whereas relatively few studies have investigated the relationships among NDVI, VOD, and model-derived GPP simultaneously. Recent studies have suggested that VOD provides complementary information to optical vegetation indices and may improve interpretations of long-term ecosystem dynamics (Dou et al., 2023). However, differences in interannual variability among vegetation indicators have received less attention than long-term trends. In addition, comprehensive assessments of how model-derived vegetation activity reproduces observation-based vegetation dynamics remain insufficient, especially across climatically and ecologically diverse regions such as Asia–Oceania. Because this region includes ecosystems ranging from tropical forests and monsoon regions to drylands and high-latitude tundra, it provides an ideal framework for evaluating indicator-dependent differences in vegetation dynamics.

This study aims to evaluate the consistency and discrepancy among multiple vegetation indicators across the Asia–Oceania region using optical, microwave, and model-based datasets. Specifically, we analyzed two NDVI datasets, microwave-based VOD, and GPP derived from the process-based ecosystem model VISIT for the period 2000–2021. We compared both long-term trends and interannual variability among indicators to assess how differences in observation principles and ecosystem sensitivities influence vegetation change assessments. The objectives of this study were to investigate (1) the extent to which vegetation indicators based on different observation principles exhibit consistent or inconsistent variability across regions, and (2) the extent to which model-derived GPP reproduces vegetation dynamics observed by satellite-based indicators. By integrating optical, microwave, and model-based information, this study highlights the importance of multi-indicator approaches for robust monitoring of terrestrial ecosystem change.

2 Materials and Methods

2.1 Study Area

The Asia–Oceania region (60°E–180°, 60°S–90°N) was selected as the study domain because its exceptional diversity of climate zones and ecosystem types provides an ideal framework for evaluating the consistency and divergence of multiple vegetation indicators. This region spans a wide range of climate zones, from tropical to polar, and includes diverse ecosystems such as forests, grasslands, arid lands, and tundra. Vegetation dynamics in this region exhibit strong spatial heterogeneity and temporal variability, making it a key component of the global carbon cycle. Recent studies have reported pronounced vegetation changes driven by climate variability, land-use change, phenological shifts, and disturbances such as droughts and wildfires. The diversity of climate and ecosystem conditions makes this region suitable for evaluating the consistency of vegetation indicators derived from different observation and estimation approaches. A systematic comparison across this heterogeneous domain enables identification of spatial patterns of agreement and disagreement among indicators.

https://doi.org/10.5194/egusphere-2026-3311
Preprint. Discussion started: 30 June 2026

2.2 Datasets

This study integrates vegetation indicators derived from optical remote sensing, microwave observations, and process-based modeling. For optical vegetation monitoring, NDVI was used, and two independent datasets were employed to enable assessment of product-level consistency and to distinguish robust vegetation signals from processing-related artifacts. The first is the SNU NDVI product provided by Seoul National University, a long-term global NDVI dataset generated by harmonizing AVHRR and MODIS observations with consistent inter-sensor calibration (Jeong et al., 2024). The second is NDVI calculated from the MODIS MCD43A4 Nadir BRDF-Adjusted Reflectance product (500 m resolution), which applies bidirectional reflectance distribution function (BRDF) corrections for more standardized comparisons across viewing and illumination angles. These two products differ in sensor origin, temporal coverage, and atmospheric correction methods; comparing them allows evaluation of how processing choices affect the inferred vegetation dynamics. Vegetation Optical Depth (VOD) was used as a microwave-based indicator sensitive to vegetation water content and aboveground biomass. The VODCA CXKu dataset (Zotta et al., 2024) was employed, which integrates passive microwave observations across C-, X-, and Ku-bands from multiple sensors into a harmonized long-term record spanning 1987–2021. Gross Primary Production (GPP) was derived from the process-based terrestrial ecosystem model VISIT (Ito and Inatomi, 2012). The model uses climate inputs from the CRU TS4.09 dataset (Harris et al., 2020; temperature, precipitation, vapor pressure, and cloud cover at 0.5° resolution) and atmospheric CO2 concentration based on RCP scenarios, enabling simulation of vegetation carbon uptake under changing climate and CO2 conditions. Regional analyses were conducted using land masks defined by the RECCAP2 project (Ciais et al., 2022). Monthly mean air temperature from the CRU TS4.09 dataset (0.5° resolution) was used to define the growing season as described in Sect. 2.3.

2.3 Data Processing

To ensure comparability among datasets derived from different observation principles and model simulations, all variables were harmonized in both spatial and temporal domains, with processing strategies adapted to the specific characteristics of each dataset. Spatial resolution varied across datasets, with SNU NDVI at 0.05°, MODIS NDVI (MCD43A4) at approximately 500 m, VOD at 0.25°, and VISIT GPP at 0.5°. For analyses focusing on individual indicators, the original spatial resolution was retained to preserve inherent spatial detail. For pairwise comparisons between indicators, datasets were resampled to the coarser resolution of each pair: 0.25° for comparisons involving VOD, and 0.5° for comparisons involving VISIT GPP, to ensure spatial consistency and minimize mismatches arising from sub-pixel heterogeneity. For regional analyses of interannual variability, spatial averaging was performed within predefined RECCAP2 regions, and the influence of resolution differences was therefore considered negligible.

All datasets were temporally aggregated to annual values to facilitate the analysis of long-term trends and interannual variability, with indicator-specific strategies adopted to minimize contamination from non-vegetation signals. The growing

https://doi.org/10.5194/egusphere-2026-3311
Preprint. Discussion started: 30 June 2026

season (GS) was defined for each grid cell and calendar month as the period when the long-term mean air temperature (1982–2024) was equal to or greater than 0°C and the corresponding long-term mean NDVI exceeded 0.1. Although this threshold-based definition is empirical, it provides a consistent criterion applicable across diverse climatic regions. For NDVI, the GS mask was applied to monthly data prior to annual averaging to focus on periods of active vegetation growth. For VOD, a peak-season sampling approach was adopted rather than annual averaging, given its sensitivity to soil moisture, freeze–thaw processes, and snow cover, particularly in high-latitude regions. Specifically, for each grid cell, the month of maximum long-term mean NDVI was identified, and the corresponding monthly VOD value was extracted for each year as a representative measure; this approach follows the widely adopted assumption that VOD during the peak growing season is least affected by frozen soil and snow and therefore most reliably reflects vegetation water content and biomass. For GPP, annual averages were calculated without applying the GS mask, because environmental constraints such as temperature, radiation, and phenology are inherently represented within the VISIT model framework, and applying an external GS mask could introduce inconsistencies with the model's internal representation of vegetation activity; annual GPP also enables a comprehensive assessment of total ecosystem carbon uptake.

Masking procedures were applied to ensure consistency in spatial and temporal coverage across all analyses. The GS mask was used to extract periods of active vegetation growth for NDVI, thereby reducing contamination from dormant or snow-covered periods that could otherwise bias annual statistics. Regional analyses were conducted using land masks defined by the RECCAP2 framework, which provides a carbon-cycle-oriented regional partition suitable for comparing vegetation dynamics across climatically and ecologically distinct zones. These masks enabled aggregation of data at the regional scale and facilitated interpretation of indicator-dependent differences within a consistent biogeochemical context.

2.4 Analysis

To evaluate the consistency and divergence among vegetation indicators, analyses were conducted from two complementary perspectives: long-term trends and interannual variability. Long-term trends were quantified for each grid cell using the non-parametric Mann–Kendall test (Mann, 1945) in combination with Sen's slope estimator (Sen, 1968). This approach was selected because it provides a robust assessment of monotonic trends that is insensitive to outliers and non-normal data distributions, making it well suited for vegetation time series that may contain episodic anomalies associated with extreme climate events or data gaps. Statistical significance was evaluated at the 0.05 level ($p < 0.05$), and only grid cells with statistically significant trends were highlighted in the spatial maps to distinguish robust signals from background variability. Trend mismatch between indicator pairs was identified when the signs of Sen's slope differed, indicating opposite directions of long-term change, and the spatial extent of agreement and disagreement was mapped across the study domain.

Interannual variability (IAV) was analyzed after removing the influence of long-term trends to isolate short-term climate-driven fluctuations. Monthly data were first filtered using the growing season (GS) mask and aggregated to annual values.

https://doi.org/10.5194/egusphere-2026-3311
Preprint. Discussion started: 30 June 2026

Spatial averaging was then performed based on RECCAP2 regions, with additional longitudinal subdivisions where appropriate to capture regional heterogeneity. The resulting time series were standardized to zero mean and unit variance (Z-score normalization) and subsequently detrended using linear regression, enabling consistent comparison of variability across indicators and regions with different mean states and magnitudes. The degree of co-variability between indicator pairs was quantified using the coefficient of determination (r^2), calculated from the detrended and standardized annual anomalies, with statistical significance assessed using a two-sided test at $p < 0.05$. Variability mismatch was defined when the correlation between indicators was not statistically significant ($p \geq 0.05$) or when r^2 fell below 0.3, indicating weak or negligible co-variability. Comparisons among indicators were conducted from three complementary viewpoints: (1) spatial patterns of long-term trends, (2) temporal patterns of interannual variability, and (3) the degree of co-variability quantified by r^2, allowing a multi-faceted assessment of indicator-dependent differences in vegetation dynamics.

To attribute GPP variability to specific environmental drivers and thereby interpret the discrepancies identified between model-derived GPP and satellite-based indicators, a series of sensitivity experiments with the VISIT model was conducted. In these experiments, individual climate drivers — precipitation, temperature, vapor pressure, and cloud cover — were varied one at a time while holding all other drivers constant at their long-term mean values, following an approach analogous to factorial simulation designs used in previous terrestrial carbon cycle studies. An additional simulation in which all climate drivers were varied simultaneously (ALLCON) was used to assess the combined climate contribution. The contribution of rising atmospheric CO_2 concentration was evaluated separately by prescribing temporally varying CO_2 while fixing climate at its long-term mean. Regional GPP was calculated as an area-weighted combination of cropland and natural vegetation components based on land cover fractions, enabling the evaluation of how climatic factors and CO_2 concentration jointly or independently drive both long-term trends and interannual variability in modeled GPP across the diverse ecosystems of the study region.

3 Results

3.1 Spatial patterns of long-term vegetation trends

Vegetation trends during 2000–2021 differed substantially among indicators across the Asia–Oceania region, with consistent greening in optical indices contrasting with spatially heterogeneous patterns in microwave-based and model-derived products (Fig. 1). Both MODIS NDVI and SNU NDVI exhibited widespread and statistically significant positive trends ($p < 0.05$) across eastern China, the Korean Peninsula, South Asia, and high-latitude regions including Siberia, reflecting pervasive greening over the study period. Positive trends in NDVI were particularly pronounced in agriculturally intensified areas of eastern China and India, where land management practices such as increased cropping intensity and irrigation are well

https://doi.org/10.5194/egusphere-2026-3311
Preprint. Discussion started: 30 June 2026

documented. In Australia, positive and negative trends coexisted locally, reflecting the high sensitivity of dryland vegetation to interannual precipitation variability.

VOD showed broadly positive trends consistent in sign with NDVI trends in East Asia and South Asia, but diverged substantially in spatial extent and magnitude in high-latitude regions. In parts of inland Siberia and Central Asia, negative VOD trends were observed in areas where both NDVI datasets indicated statistically significant greening, resulting in noticeable spatial discrepancies. This divergence between VOD and NDVI likely reflects fundamental differences in the vegetation properties captured by each indicator: while NDVI responds primarily to canopy greenness and optical properties, VOD is sensitive to vegetation water content and aboveground biomass, which may respond differently to environmental changes in temperature-limited ecosystems.

VISIT-derived GPP exhibited particularly strong positive trends over South Asia, exceeding the magnitude of NDVI trends in that region. In boreal regions such as Siberia, however, GPP showed largely non-significant trends despite the widespread greening indicated by both NDVI datasets, resulting in a clear spatial divergence between NDVI and GPP. The magnitude of both positive and negative GPP trends was larger than in the satellite-based indicators across several regions, suggesting that the process-based model amplifies trend signals associated with climatic and CO_2 forcing. These results indicate that vegetation trends inferred from optical, microwave, and model-based indicators are not spatially consistent across all ecosystem types and climatic regions.

https://doi.org/10.5194/egusphere-2026-3311
Preprint. Discussion started: 30 June 2026

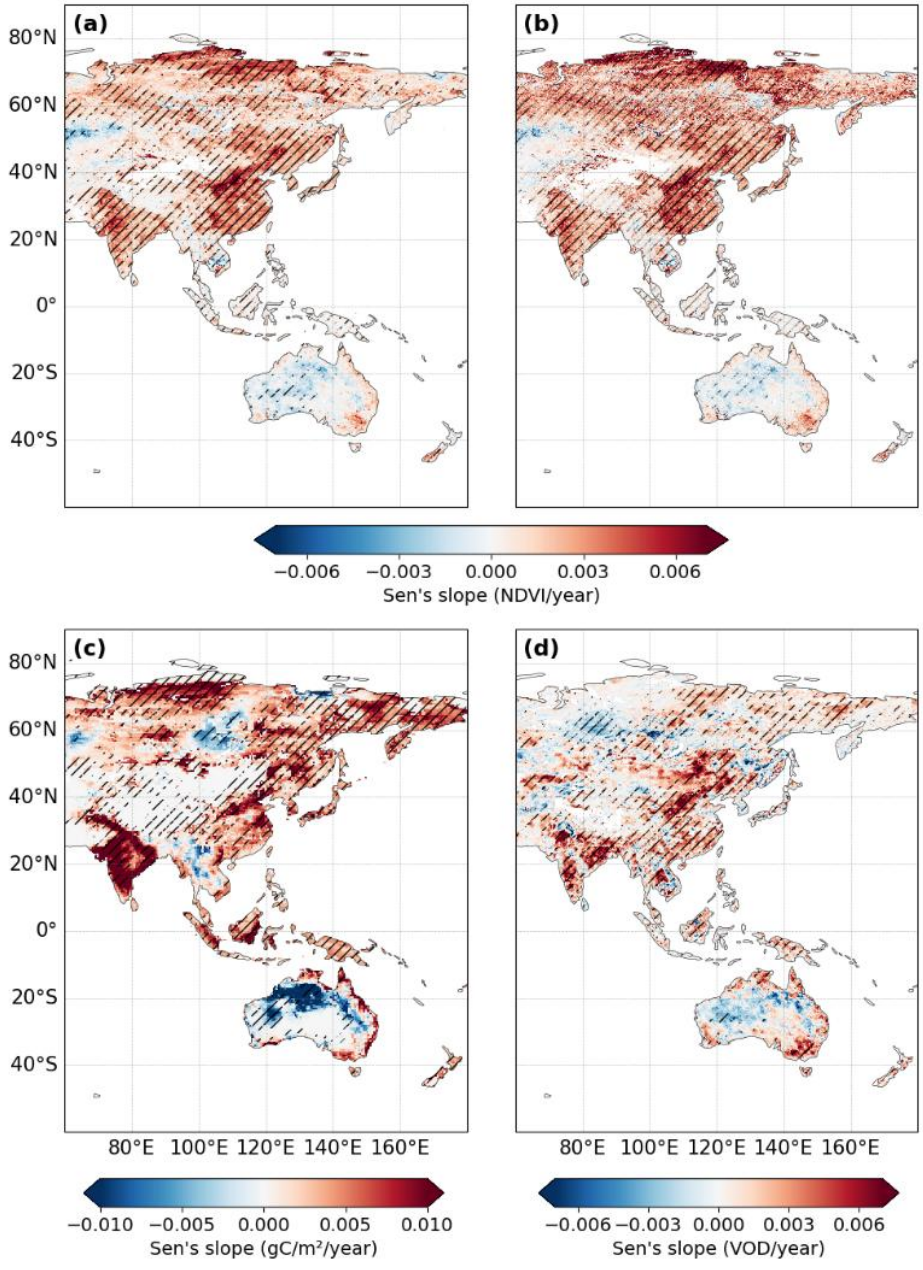

Figure 1. Spatial distribution of long-term trends (2000–2021) for each vegetation indicator. Trends were calculated using Sen's slope based on mean annual values of (a) MODIS NDVI, (b) SNU NDVI, (c) VOD, and (d) GPP derived from the VISIT model. Statistically significant trends ($p < 0.05$) based on the Mann–Kendall test are indicated by hatching.

https://doi.org/10.5194/egusphere-2026-3311
Preprint. Discussion started: 30 June 2026

3.2 Interannual variability and trend agreement among satellite indicators

The degree of interannual variability (IAV) agreement among vegetation indicators was strongly dependent on the indicator pair considered, with high consistency between the two NDVI datasets but substantially lower coherence between optical and microwave-based indicators across most regions (Fig. 2). Pixel-wise r^2 values between SNU NDVI and MODIS NDVI were generally high (> 0.6–0.8) across large areas of China, South Asia, and Australia, indicating consistent year-to-year vegetation fluctuations between the two optical products. In contrast, r^2 values between NDVI and VOD were substantially lower across most regions, often below 0.2, with near-zero correlations particularly evident in Siberia and tropical Southeast Asia. In Central Asia, r^2 between NDVI and VOD was relatively higher compared to other regions. When GPP was compared with satellite-based indicators, moderate r^2 values were observed in Australia and South Asia, while large areas of low correlation ($r^2 < 0.4$) were found on the Tibetan Plateau and in tropical Southeast Asia (Fig. 5).

Trend agreement maps revealed spatial patterns of consistency and disagreement that were distinct from IAV agreement patterns, demonstrating that short-term and long-term dynamics of vegetation indicators do not necessarily co-vary (Figs. 3 and 6). Between the two NDVI datasets, widespread greening agreement was observed across the study domain, broadly consistent with their high IAV correlations. However, comparing NDVI with VOD revealed extensive disagreement in high-latitude regions, where the two indicators exhibited opposite trend signs despite moderate IAV correlations in Central Asia. In the comparison between NDVI and VISIT GPP, dominant greening agreement was observed in South and East Asia, while disagreement patterns were widespread in parts of Southeast Asia, Siberia, and Central Asia, where NDVI indicated greening but GPP showed negative or non-significant trends. These results indicate that agreement in IAV does not guarantee agreement in long-term trends, underscoring the importance of evaluating both temporal dimensions when comparing vegetation indicators.

https://doi.org/10.5194/egusphere-2026-3311
Preprint. Discussion started: 30 June 2026

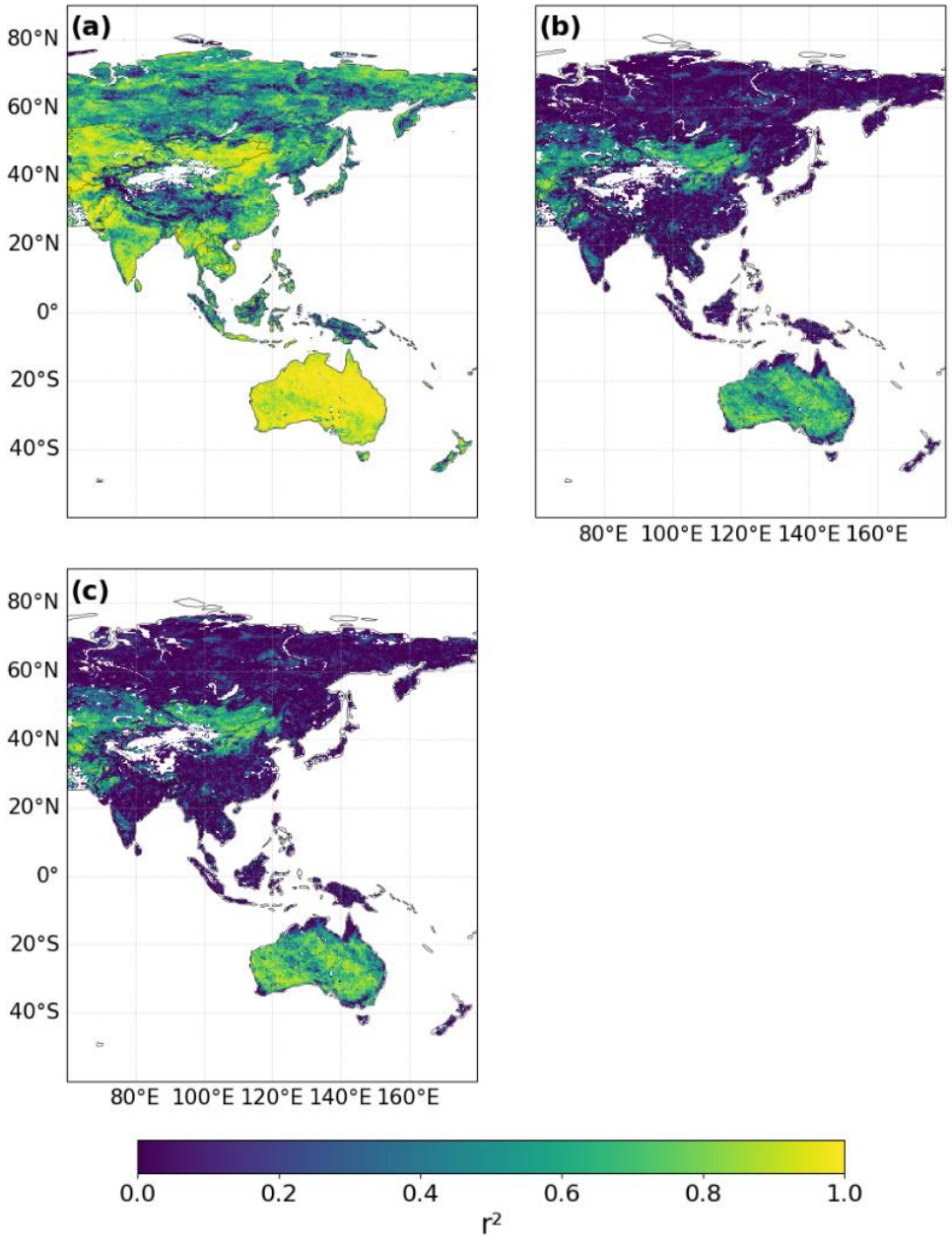

240 **Figure 2. Spatial patterns of interannual variability agreement expressed as the coefficient of determination (r^2) between (a) SNU NDVI and MODIS NDVI, (b) SNU NDVI and VOD, and (c) MODIS NDVI and VOD for the period 2000–2021. All datasets were aggregated to a common spatial resolution of 0.25° prior to comparison. The r^2 values were calculated from detrended and standardized annual anomalies. Higher r^2 values indicate stronger agreement in interannual variability. Only the Asia–Oceania region (60°E–180°E, 60°S–90°N) is shown.**

https://doi.org/10.5194/egusphere-2026-3311
Preprint. Discussion started: 30 June 2026

245

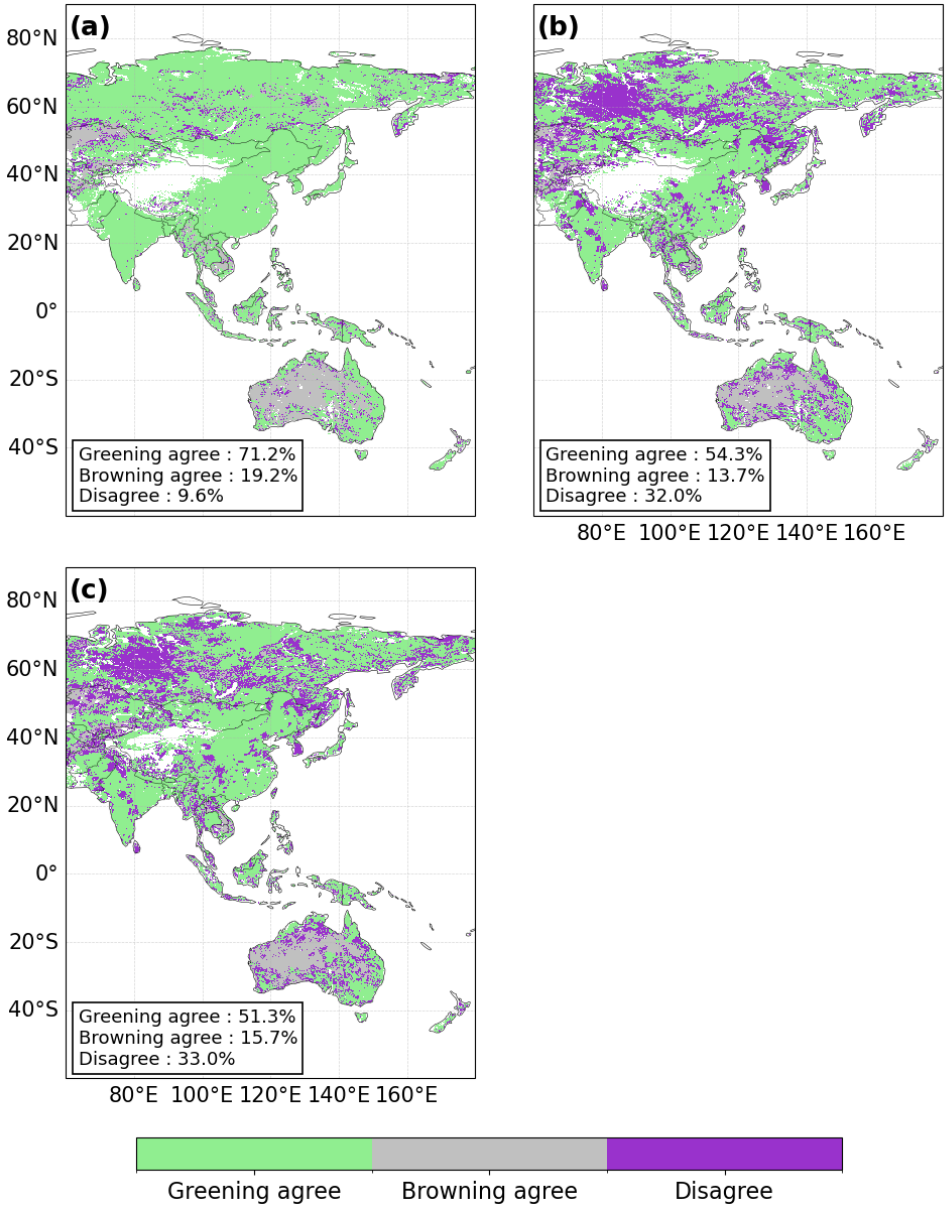

Figure 3. Spatial patterns showing the consistency of long-term trends among vegetation indicators from 2000 to 2021: (a) SNU NDVI vs. MODIS NDVI, (b) SNU NDVI vs. VOD, and (c) MODIS NDVI vs. VOD. Trends are classified into 250 **three categories: agreement in positive trends ("greening agreement"), agreement in negative trends ("browning agreement"), and disagreement (opposite trend signs). All datasets were resampled to a common spatial resolution of 0.25° prior to comparison. The analysis area is limited to the Asia–Oceania region (60°–180° E, 60° S–90° N).**

https://doi.org/10.5194/egusphere-2026-3311
Preprint. Discussion started: 30 June 2026

3.3 Regional differences in interannual variability

Regional analyses of interannual variability revealed systematic indicator-dependent differences that varied with climatic and ecosystem characteristics, with strong coherence in precipitation-limited regions but substantial divergence in boreal and tropical ecosystems (Fig. 4). High agreement among all indicator pairs was observed in Central Asia and Australia, where r^2 values exceeded 0.70 for all pairwise combinations, indicating that year-to-year vegetation fluctuations were consistently captured by optical, microwave, and model-based indicators. These regions are characterized by strong precipitation-driven variability, which provides a dominant and coherent hydroclimatic forcing across all indicator types.

In contrast, Siberia showed only moderate correlation between SNU NDVI and MODIS NDVI ($r^2 = 0.413$), while correlations with VOD were near zero (SNU NDVI–VOD: $r^2 = 0.025$; MODIS NDVI–VOD: $r^2 = 0.022$), indicating that the three indicators captured largely independent interannual signals in this temperature-limited boreal region. In the monsoon-dominated regions of South Asia and Southeast Asia, NDVI pairs showed relatively high mutual correlations ($r^2 = 0.739$–0.963), confirming the consistency of optical vegetation signals across these products. However, correlations between NDVI and VOD in these regions remained low ($r^2 = 0.060$–0.199), suggesting that microwave-derived vegetation water content did not co-vary with optical greenness on interannual timescales. These results demonstrate that indicator agreement depends strongly on both the regional climate regime and the physical property each indicator measures.

https://doi.org/10.5194/egusphere-2026-3311
Preprint. Discussion started: 30 June 2026

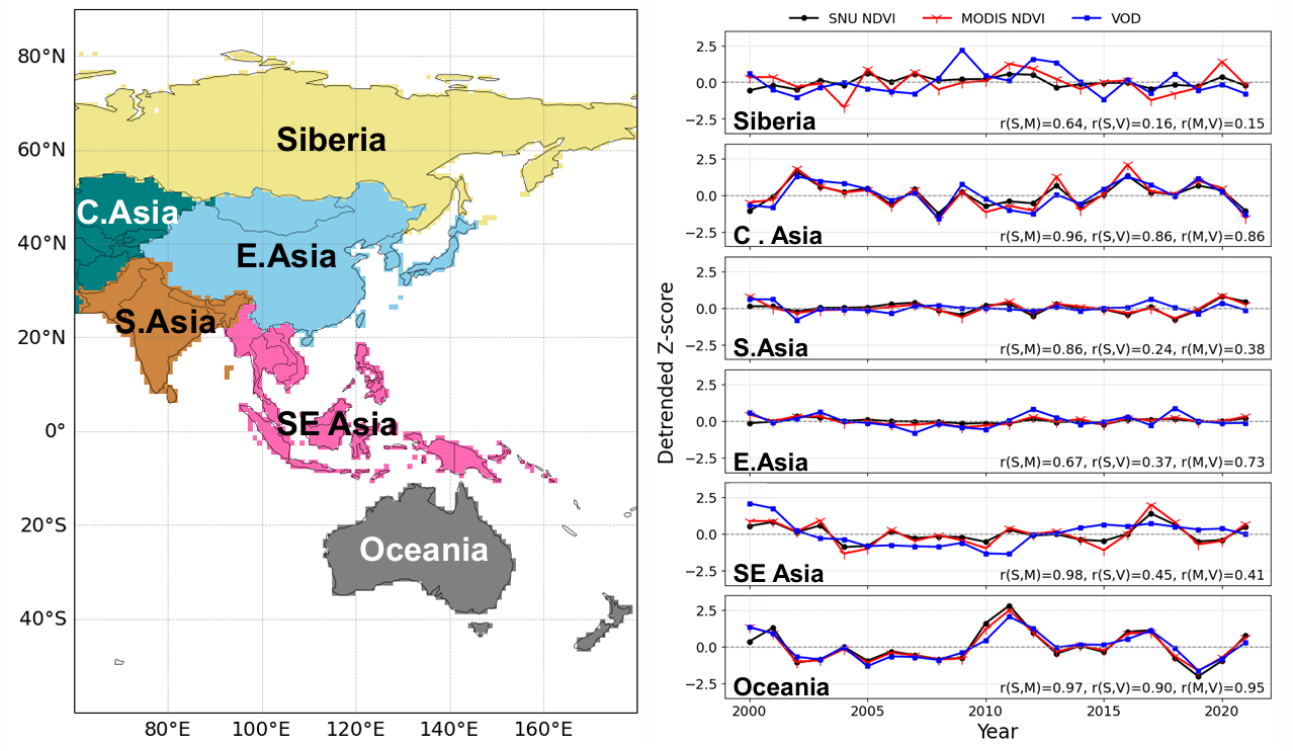

Figure 4. Time series of detrended anomalies of NDVI and VOD averaged over RECCAP2 regions for the period 2000–2021. Panels show (a) Siberia, (b) Central Asia, (c) South Asia, (d) East Asia, (e) Southeast Asia, and (f) Oceania. Black lines (S) indicate SNU NDVI, red lines (M) indicate MODIS NDVI, and blue lines (V) indicate VOD. All time series are detrended and standardized anomalies to highlight interannual variability. The zero line represents the long-term mean. Values of r between indicator pairs are shown in each panel.

3.4 Comparison between satellite-based indicators and model-derived GPP

VISIT-derived GPP reproduced broad spatial and temporal patterns of vegetation variability but showed systematic regional discrepancies relative to satellite-based indicators, particularly in high-latitude boreal and tropical regions (Figs. 5 and 6). Moderate r^2 values between GPP and NDVI were found in Australia and South Asia, regions where interannual variability is strongly driven by precipitation, suggesting that the process-based model captures the dominant climatic controls on vegetation carbon uptake in precipitation-limited ecosystems. In East Asia, the consistency among NDVI, VOD, and GPP suggests that vegetation increases were supported by both observation-based and model-based indicators.

However, large areas with r^2 below 0.4 were observed on the Tibetan Plateau and in tropical Southeast Asia when GPP was compared with both NDVI datasets. Correlations between GPP and VOD were even lower than those between GPP and NDVI

https://doi.org/10.5194/egusphere-2026-3311
Preprint. Discussion started: 30 June 2026

across most regions, with widespread spatial disagreement particularly in high-latitude regions where soil moisture and freeze–thaw dynamics may introduce signals unrelated to vegetation carbon uptake. Trend agreement maps showed dominant greening agreement between GPP and NDVI in South and East Asia, while disagreement patterns were extensive in parts of Southeast Asia, Siberia, and Central Asia, where NDVI indicated greening but VISIT GPP showed negative or non-significant trends. These discrepancies suggest that the process-based model does not fully reproduce the processes driving optical greening trends in boreal and tropical environments, potentially including structural changes in leaf area or land management effects not represented in the model.

Overall, the comparison between satellite-based indicators and model-derived GPP demonstrated that no single indicator fully represents all aspects of vegetation dynamics across the Asia–Oceania region. The distinct sensitivities of optical, microwave, and model-based indicators to vegetation structure, water status, and environmental forcing collectively produce a regionally differentiated picture of ecosystem change that cannot be captured by any single approach alone.

https://doi.org/10.5194/egusphere-2026-3311
Preprint. Discussion started: 30 June 2026

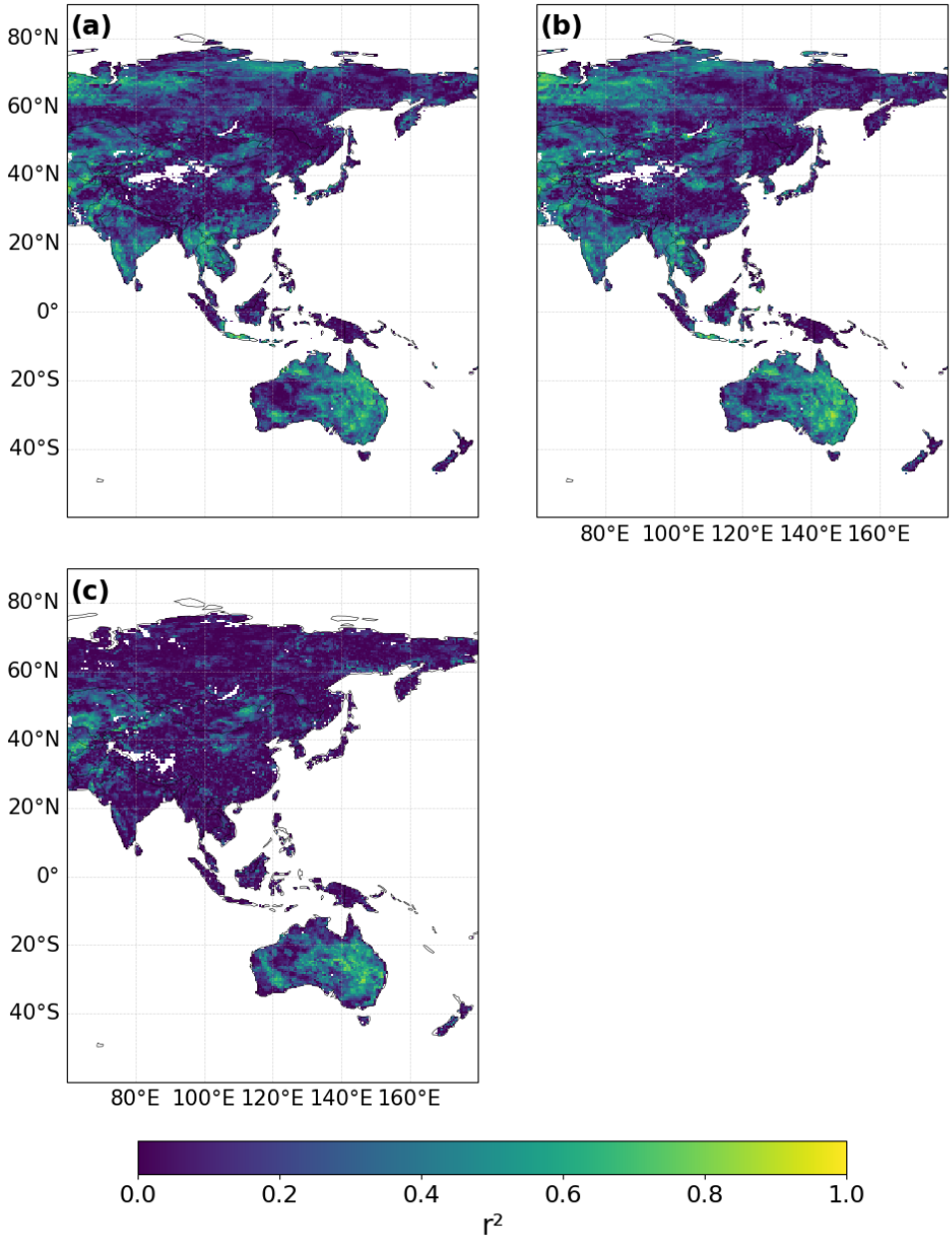

Figure 5. Spatial patterns of interannual variability agreement expressed as the coefficient of determination (r^2) between (a) SNU NDVI and VISIT GPP, (b) MODIS NDVI and VISIT GPP, and (c) VOD and VISIT GPP for the period 2000–2021. All datasets were aggregated to a common spatial resolution of 0.25° prior to comparison. The r^2 values were calculated from detrended and standardized annual anomalies. Higher r^2 values indicate stronger agreement in interannual variability. Only the Asia–Oceania region (60°E–180°E, 60°S–90°N) is shown.

https://doi.org/10.5194/egusphere-2026-3311
Preprint. Discussion started: 30 June 2026

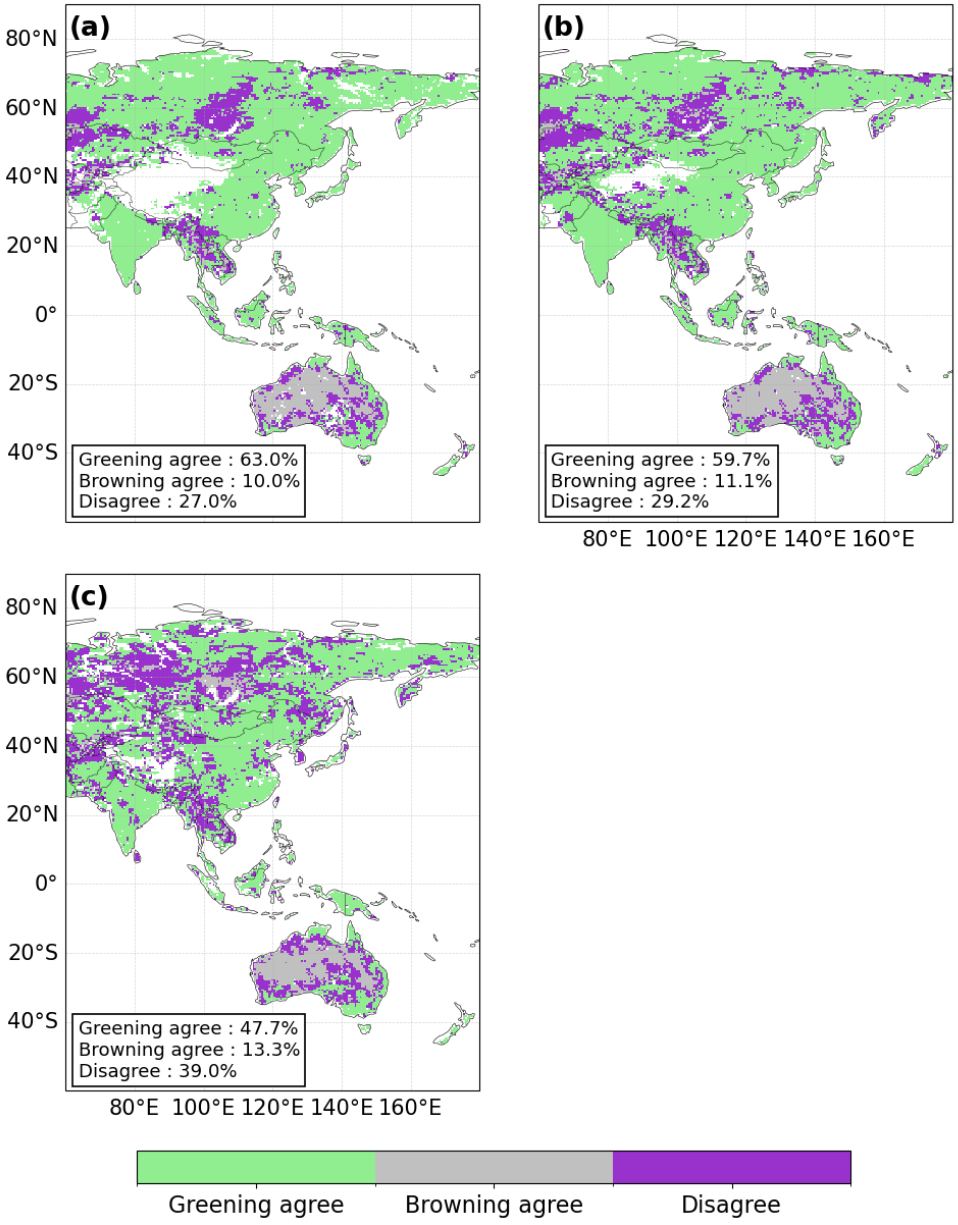

315 **Figure 6. Spatial patterns showing the consistency of long-term trends among vegetation indicators from 2000 to 2021: (a) SNU NDVI vs. VISIT GPP, (b) MODIS NDVI vs. VISIT GPP, and (c) VOD vs. VISIT GPP. Trends are classified into three categories: agreement in positive trends ("greening agreement"), agreement in negative trends ("browning agreement"), and disagreement (opposite trend signs). All datasets were resampled to a common spatial resolution of 0.25° prior to comparison. The analysis area is limited to the Asia–Oceania region (60°–180° E, 60° S–90° N).**

320

https://doi.org/10.5194/egusphere-2026-3311
Preprint. Discussion started: 30 June 2026

3.5 Attribution of GPP variability to climate drivers and CO2

To understand the mechanisms underlying regional discrepancies between model-derived GPP and satellite-based indicators, sensitivity experiments with the VISIT model were conducted to attribute GPP variability to individual climate drivers and atmospheric CO_2 concentration, providing a process-level perspective on the drivers of modeled vegetation dynamics (Fig. 7). The CO_2 scenario produced a consistent and gradual positive trend in GPP across all regions, confirming that rising atmospheric CO_2 was the primary driver of the long-term GPP increases simulated by VISIT. In contrast, interannual variability in GPP was dominated by climate forcing, with regionally distinct patterns among climate drivers.

Climate drivers of GPP variability showed distinct regional characteristics, with precipitation dominant in Australia, temperature more influential in Siberia, and vapor pressure important in South and Central Asia. In Australia, precipitation variability closely tracked GPP interannual variability, identifying precipitation as the dominant driver in this dryland-dominated region, consistent with the high IAV agreement between GPP and satellite-based indicators found there. In Central Asia and South Asia, contributions from vapor pressure and precipitation were both prominent, reflecting the combined influence of water availability and atmospheric demand on ecosystem carbon uptake. In Siberia, temperature exerted a relatively larger role in controlling GPP variability, consistent with the temperature-limited nature of boreal ecosystem productivity. In Southeast Asia, interannual variability in all climate drivers was comparatively small, and GPP variability was correspondingly limited, which may partly explain the low r^2 values between GPP and satellite-based indicators in that region. Across all regions, raw GPP showed larger interannual variability than the ALLCON simulation, indicating non-linear interactions among climate drivers. These results highlight that the controls on GPP variability are strongly region-specific, and that discrepancies between model-derived and observation-based indicators partly reflect differences in the dominant environmental forcings captured by each indicator type.

https://doi.org/10.5194/egusphere-2026-3311
Preprint. Discussion started: 30 June 2026

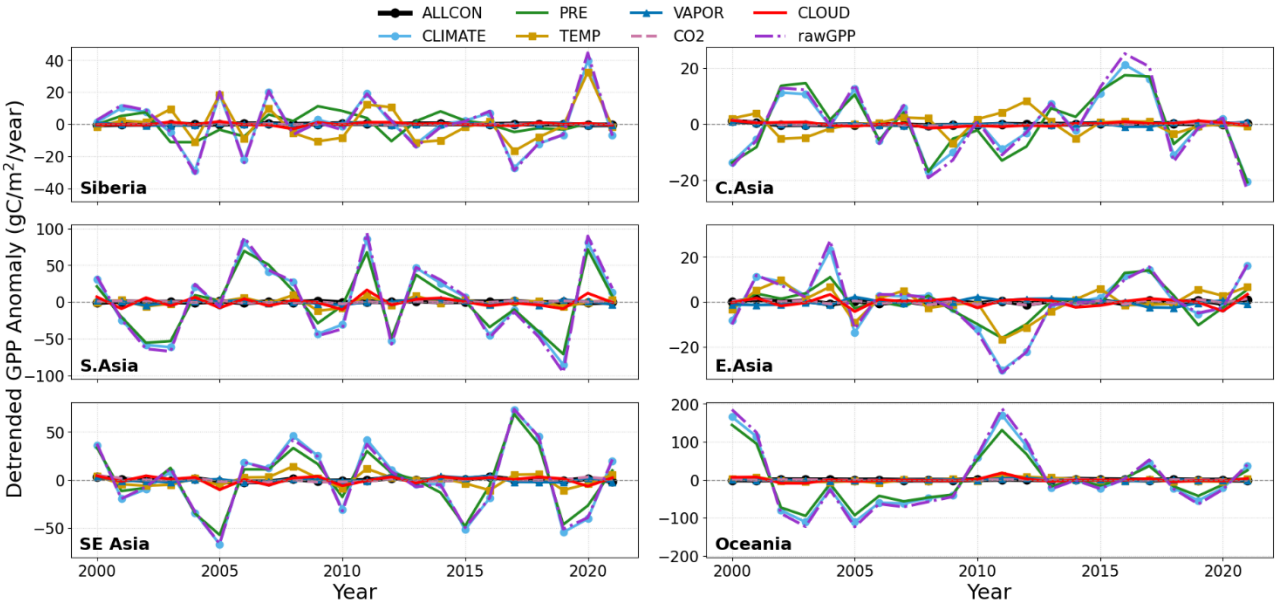

345 **Figure 7. Time series of detrended anomalies of GPP and its sensitivity components over RECCAP2 regions for 2000–2021. The lines represent the contributions from different drivers derived from VISIT sensitivity experiments: ALLCON (all climate drivers combined), CLIMATE (total climate contribution), PRE (precipitation), TEMP (temperature), VAPOR (vapor pressure), CLOUD (cloud cover), and CO_2 (atmospheric CO_2 concentration), along with the original GPP (rawGPP). All series are expressed as anomalies relative to the 2000–2021 mean. Differences in**
350 **amplitude among panels reflect regional differences in GPP sensitivity to climate drivers.**

4 Discussions

4.1 Causes of inconsistencies among indicators across temporal scales

The inconsistencies among NDVI, VOD, and GPP identified in this study cannot be attributed to observational noise but
355 instead arise from fundamental differences in the vegetation properties each indicator captures. NDVI primarily reflects canopy greenness and optical properties, responding to changes in chlorophyll content and leaf area. VOD is sensitive to vegetation water content and aboveground biomass, integrating signals from both the canopy and sub-canopy layers. GPP represents carbon assimilation and reflects the physiological capacity of vegetation to fix atmospheric CO_2 under prevailing environmental conditions. Because these indicators track different components of ecosystem state and function — structure,
360 water status, and carbon uptake, respectively — they are not expected to respond linearly or synchronously to the same environmental forcing. Consequently, increases in NDVI do not necessarily correspond to increases in biomass or carbon uptake, and VOD may respond strongly to changes in water availability while NDVI remains relatively stable. The

https://doi.org/10.5194/egusphere-2026-3311
Preprint. Discussion started: 30 June 2026

inconsistencies identified in this study therefore reflect nonlinear and asynchronous responses of different vegetation components rather than errors in any individual dataset, and assessments based on a single indicator will inevitably emphasize only one dimension of ecosystem dynamics.

Importantly, the nature of these inconsistencies differs systematically between long-term trends and interannual variability, reflecting the distinct environmental controls that operate at each timescale. Long-term trends primarily reflect sustained changes in vegetation structure or ecosystem function driven by decadal-scale forcing such as rising atmospheric CO_2, land-use management, or progressive climate change. In contrast, interannual variability captures short-term responses to climate fluctuations, and the dominant controls on these fluctuations differ markedly among indicators. NDVI responds rapidly to changes in canopy greenness associated with temperature and precipitation seasonality, whereas VOD tracks vegetation water content and may react more immediately to short-term moisture availability following precipitation events. GPP is jointly controlled by radiation, temperature, and CO_2 concentration, leading to temporal patterns that can diverge from both optical and microwave indicators even when long-term trends are broadly consistent. This dual-timescale perspective explains why regions with agreement in long-term trends — such as East Asia — can simultaneously exhibit low correlations in interannual variability between NDVI and VOD, and why the spatial patterns of trend agreement and IAV agreement do not necessarily coincide across the study domain. Inconsistencies in interannual variability therefore should not be dismissed as noise but instead reflect the existence of distinct ecological processes operating at short timescales, providing complementary and meaningful information for understanding ecosystem dynamics beyond what trend analyses alone can reveal. A multi-indicator approach integrating optical, microwave, and model-based information is therefore essential for capturing the full complexity of vegetation responses across both temporal dimensions.

4.2 Climatic, ecosystem, and model-structural controls on spatial patterns of inconsistency

The spatial distribution of inconsistencies among indicators shows systematic patterns closely linked to climate conditions, ecosystem characteristics, and the structural limitations of the process-based model. In high-latitude regions, the disagreement between VOD and the other indicators is largely attributable to the sensitivity of microwave observations to soil moisture, freeze–thaw dynamics, and snow cover, which introduce signals unrelated to vegetation activity that persist even after seasonal filtering. In temperature-limited boreal ecosystems, NDVI and GPP primarily respond to temperature variability, whereas VOD is additionally influenced by hydrological conditions, creating divergent temporal and long-term patterns. This divergence is particularly pronounced in the West Siberian Lowland, where extensive wetlands and peatlands maintain high and variable soil moisture year-round. Under such conditions, changes in soil dielectric properties strongly contaminate microwave signals, rendering the separation of vegetation and soil contributions in VOD retrieval incomplete. The relatively high-frequency microwave signals of the VODCA CXKu dataset further amplify surface effects in sparsely vegetated or wetland environments, and uncertainties in land cover classification over these regions may additionally introduce apparent variability unrelated to actual vegetation change.

https://doi.org/10.5194/egusphere-2026-3311
Preprint. Discussion started: 30 June 2026

In dry and semi-arid regions, inconsistencies are primarily driven by differences in the temporal responses of indicators to precipitation variability. VOD responds rapidly to changes in vegetation water content following rainfall events, whereas NDVI depends on leaf development and canopy structural changes that may introduce time lags or threshold responses relative to precipitation. These differences reduce the coherence of interannual variability between the two indicators even in regions where both show broadly positive long-term trends. In high-biomass forest regions, NDVI saturation further limits its sensitivity to structural changes, whereas VOD and GPP maintain a wider dynamic range, contributing to additional spatial inconsistencies particularly in tropical Southeast Asia. Overall, inconsistencies among indicators emerge from the combined effects of climate regime, ecosystem structure, observation principles, soil moisture variability, and land cover uncertainty, and no single factor is sufficient to explain the full spatial pattern of disagreement across the Asia–Oceania region.

The regional discrepancies between VISIT-derived GPP and satellite-based indicators reflect not only model structural limitations but also a fundamental difference in the observational targets of model outputs and remote sensing products. While VISIT captures the response of vegetation carbon uptake to climate drivers and CO_2 concentration and reproduces broad spatial patterns of vegetation productivity, it does not fully represent local controls such as water limitation, soil heterogeneity, vegetation structural changes, or land-use effects including irrigation and cropping intensity. These processes are known to drive optical greening trends in agriculturally intensified regions of East and South Asia, and their absence from the model contributes to the discrepancies between GPP and NDVI trends in parts of these regions. More fundamentally, GPP represents a functional response variable, whereas NDVI and VOD capture structural and state variables of the canopy; this inherent difference in observational target introduces a gap between model and satellite indicators that should not be interpreted solely as model error. Reducing this gap will require the integration of observation-based constraints — such as satellite-derived LAI, SIF, or VOD — into the model forcing or validation framework, alongside improved representation of hydrological and land-management processes.

4.3 Uncertainties and methodological limitations

The analytical choices made in this study — particularly the growing season definition and the peak-season sampling approach for VOD — introduce region-specific uncertainties that should be considered when interpreting spatial and temporal patterns of indicator agreement. The growing season definition, based on long-term mean air temperature (≥ 0°C) and NDVI (≥ 0.1) thresholds, provides a consistent and reproducible criterion applicable across diverse climatic regions, but remains empirical and may not optimally capture the onset and cessation of vegetation activity in all ecosystems. In particular, the peak-season sampling approach adopted for VOD may introduce temporal bias in regions where the month of maximum NDVI does not coincide with the period of maximum vegetation water content or biomass development. Spatial aggregation and resolution harmonization, while necessary for pairwise comparisons, may smooth local variability and reduce the sensitivity of comparisons at fine spatial scales. Furthermore, the coefficient of determination (r^2) used to evaluate interannual variability

https://doi.org/10.5194/egusphere-2026-3311
Preprint. Discussion started: 30 June 2026

agreement is sensitive to time series length; the 22-year record used here, although sufficient for detecting dominant signals, may limit statistical power in regions with high interannual noise or infrequent extreme events.

Beyond methodological choices, uncertainties inherent in the input datasets and the VISIT model structure introduce additional limitations that affect the reliability of indicator comparisons, particularly in data-sparse or ecologically complex regions. VISIT-derived GPP contains uncertainties related to the quality of CRU TS4.09 climate inputs, model parameterization, and the exclusion of biogeochemical and land-management processes such as nitrogen cycling, irrigation, and disturbance dynamics, all of which may contribute to discrepancies between modeled and observed vegetation dynamics, particularly in intensively managed agricultural regions. Land cover classification uncertainties — particularly over the wetland-dominated regions of West Siberia — may affect the interpretation of VOD trends, as misclassification can introduce apparent temporal variability unrelated to actual vegetation change. The use of two independent NDVI datasets helps identify processing-related inconsistencies and distinguish robust signals from artifacts; however, it does not fully resolve the question of which dataset more accurately represents true vegetation dynamics in any given region, and caution is warranted when attributing discrepancies among indicators to ecological processes rather than residual data quality issues.

4.4 Implications and future perspectives

The inconsistencies identified in this study among optical, microwave, and model-based vegetation indicators represent scientifically meaningful signals rather than analytical artifacts. They reveal that vegetation structure, water status, and carbon uptake do not respond uniformly to the same environmental forcing, and that the choice of indicator critically shapes the conclusions drawn about the direction, magnitude, and spatial extent of vegetation change. This has direct implications for global carbon budget assessments, where satellite-derived greening trends have often been interpreted as evidence of enhanced carbon uptake. Our results suggest that such interpretations should be treated with caution, particularly in high-latitude and boreal regions where NDVI greening is not consistently accompanied by increases in biomass or GPP. A multi-indicator framework that integrates complementary observation types is therefore not merely advantageous but necessary for robust monitoring of terrestrial ecosystem change and its role in the global carbon cycle.

Future research should prioritize the development of frameworks that explicitly account for the differing sensitivities of vegetation indicators and leverage their complementarity rather than treating them as interchangeable. The integration of solar-induced chlorophyll fluorescence (SIF; Li and Xiao, 2019), which provides a more direct measure of photosynthetic activity than reflectance-based indices, alongside VOD and process-based model outputs, offers a promising avenue for disentangling structural, physiological, and functional responses to climate variability. In high-latitude wetland regions, where VOD signals are strongly contaminated by soil moisture and hydrological variability, dedicated retrieval algorithms that explicitly separate vegetation and surface contributions are needed. More broadly, the assimilation of multi-source satellite observations — including optical, microwave, and fluorescence data — into terrestrial ecosystem models represents a critical step toward

https://doi.org/10.5194/egusphere-2026-3311
Preprint. Discussion started: 30 June 2026

reducing the gap between observation-based and model-derived estimates of vegetation dynamics and land carbon fluxes across the diverse environments of Asia–Oceania and beyond.

5 Conclusions

This study compared long-term trends and interannual variability among two NDVI datasets, Vegetation Optical Depth (VOD), and model-derived gross primary production (GPP) across the Asia–Oceania region during 2000–2021. Although all indicators were used to monitor vegetation dynamics, they often showed different spatial and temporal patterns. Both NDVI datasets indicated widespread vegetation increases across East Asia and northern Eurasia, whereas VOD and GPP exhibited weaker and more heterogeneous responses, particularly in high-latitude regions.

The degree of agreement among indicators varied substantially among regions. East Asia showed relatively consistent positive trends and interannual variability among NDVI, VOD, and GPP, suggesting coherent changes in vegetation greenness, biomass, and ecosystem productivity. In contrast, Siberia showed large discrepancies among indicators, with strong NDVI greening not always accompanied by corresponding increases in VOD or GPP. These results suggest that vegetation changes inferred from a single indicator may not fully represent ecosystem dynamics in some regions.

Our results demonstrate that different vegetation indicators capture different aspects of ecosystem structure and function. Integrating optical, microwave, and model-based information can therefore improve the interpretation of long-term vegetation change and provide a more comprehensive understanding of ecosystem responses across the diverse environments of Asia–Oceania.

Code and data availability

The datasets used in this study are publicly available from the original data providers cited in the text. Processed data and analysis scripts are available from the corresponding author upon reasonable request.

Author contributions

MK and KI designed the experiments; MK and DH prepared the data used in this study; MK conducted the analysis. MK prepared the manuscript with supervision by KI, and contributions from all co-authors (MH, DH, and MB).

https://doi.org/10.5194/egusphere-2026-3311
Preprint. Discussion started: 30 June 2026

Competing interests

The authors declare that they have no competing interests.

Financial support

This study is supported by JSPS Kakenhi Grant Number 24H01504 and the Environment Research and Technology Development Fund (Grant Number JPMEERF24S12230) of the Environmental Restoration and Conservation Agency of Japan funded by the Ministry of the Environment.

References

Chen, C., Park, T., Wang, X., Piao, S., Xu, B., Chaturvedi, R. K., Fuchs, R., Brovkin, V., Ciais, P., Fensholt, R., Tømmervik, H., Bala, G., Zhu, Z., Nemani, R. R., and Myneni, R. B.: China and India lead in greening of the world through land-use management, Nat. Sustain., 2, 122–129, https://doi.org/10.1038/s41893-019-0220-7, 2019.

Ciais, P., Bastos, A., Chevallier, F., Lauerwald, R., Poulter, B., Canadell, J. G., Hugelius, G., Jackson, R. B., Jain, A., Jones, M., Kondo, M., Luijkx, I., Patra, P. K., Peters, W., Pongratz, J., Peregon, A., Regnier, P., Reichstein, M., Rosan, T. M., Tian, H., Yin, Y., Zhu, D., and the RECCAP2 team: Definitions and methods to estimate regional land carbon fluxes for the second phase of the REgional Carbon Cycle Assessment and Processes Project (RECCAP-2), Geosci. Model Dev., 15, 1289–1316, https://doi.org/10.5194/gmd-15-1289-2022, 2022.

Dou, Y., Tian, F., Wigneron, J.-P., Tagesson, T., Du, J., Brandt, M., Liu, Y., Zou, L., Kimball, J. S., and Fensholt, R.: Reliability of using vegetation optical depth for estimating decadal and interannual carbon dynamics, Remote Sens. Environ., 285, 113390, https://doi.org/10.1016/j.rse.2022.113390, 2023.

Forkel, M., Carvalhais, N., Rödenbeck, C., Keeling, R., Heimann, M., Thonicke, K., Zaehle, S., and Reichstein, M.: Enhanced seasonal CO2 exchange caused by amplified plant productivity in northern ecosystems, Science, 351, 696–699, https://doi.org/10.1126/science.aac4971, 2016.

Frappart, F., Wigneron, J.-P., Li, X., Liu, X., Al-Yaari, A., Fan, L., Wang, M., Liu, X., Ahmad, S., and Kerr, Y.: Global monitoring of the vegetation dynamics from the Vegetation Optical Depth (VOD): A review, Remote Sens., 12, 2915, https://doi.org/10.3390/rs12182915, 2020.

Friedlingstein, P., Jones, M. W., O'Sullivan, M., Andrew, R. M., Bakker, D. C. E., Hauck, J., Le Quéré, C., Peters, G. P., Peters, W., Pongratz, J., Sitch, S., Canadell, J. G., Ciais, P., Jackson, R. B., Alin, S. R., Anthoni, P., Bates, N. R., Becker, M., Bellouin, N., Bopp, L., Chau, T. T. T., Chevallier, F., Chini, L. P., Cronin, M., Currie, K. I., Decharme, B., Djeutchouang, L. M., Dou, X., Evans, W., Feely, R. A., Feng, L., Gasser, T., Gilfillan, D., Gkritzalis, T., Grassi, G., Gregor, L., Gruber, N., Gürses, Ö., Harris, I., Houghton, R. A., Hurtt, G. C., Iida, Y., Ilyina, T., Luijkx, I. T., Jain, A., Jones, S. D., Kato, E., Kennedy, D., Klein Goldewijk, K., Knauer, J., Korsbakken, J. I., Körtzinger, A., Landschützer, P., Lauvset, S. K., Lefèvre, N., Lienert,

https://doi.org/10.5194/egusphere-2026-3311
Preprint. Discussion started: 30 June 2026

S., Liu, J., Marland, G., McGuire, P. C., Melton, J. R., Munro, D. R., Nabel, J. E. M. S., Nakaoka, S.-I., Niwa, Y., Ono, T., Pierrot, D., Poulter, B., Rehder, G., Resplandy, L., Robertson, E., Rödenbeck, C., Rosan, T. M., Schwinger, J., Schwingshackl, C., Séférian, R., Sutton, A. J., Sweeney, C., Tanhua, T., Tans, P. P., Tian, H., Tilbrook, B., Tubiello, F., van der Werf, G. R., Vuichard, N., Wada, C., Wanninkhof, R., Watson, A. J., Willis, D., Wiltshire, A. J., Yuan, W., Yue, C., Yue, X., Zaehle, S., and Zeng, J.: Global carbon budget 2021, Earth Syst. Sci. Data, 14, 1917–2005, https://doi.org/10.5194/essd-14-1917-2022, 2022.

Harris, I., Osborn, T. J., Jones, P., and Lister, D.: Version 4 of the CRU TS monthly high-resolution gridded multivariate climate dataset, Sci. Data, 7, 109, https://doi.org/10.1038/s41597-020-0453-3, 2020.

Ito, A. and Inatomi, M.: Use of a process-based model for assessing the methane budgets of global terrestrial ecosystems and evaluation of uncertainty, Biogeosciences, 9, 759–773, https://doi.org/10.5194/bg-9-759-2012, 2012.

Jeong, S., Ryu, Y., Gentine, P., Lian, X., Fang, J., Li, X., Dechant, B., Kong, J., Choi, W., Jiang, C., Keenan, T. F., Harrison, S. P., and Prentice, I. C.: Persistent global greening over the last four decades using novel long-term vegetation index data with enhanced temporal consistency, Remote Sens. Environ., 311, 114282, https://doi.org/10.1016/j.rse.2024.114282, 2024.

Konings, A. G., Rao, K., and Steele-Dunne, S. C.: Macro to micro: microwave remote sensing of plant water content for physiology and ecology, New Phytol., 223, 1166–1172, https://doi.org/10.1111/nph.15808, 2019.

Li, X. and Xiao, J.: A global, 0.05-degree product of solar-induced chlorophyll fluorescence derived from OCO-2, MODIS, and reanalysis data, Remote Sens., 11, 517, https://doi.org/10.3390/rs11050517, 2019.

Mann, H. B.: Nonparametric tests against trend, Econometrica, 13, 245–259, https://doi.org/10.2307/1907187, 1945.

Momen, M., Wood, J. D., Novick, K. A., Pangle, R., Pockman, W. T., McDowell, N. G., and Konings, A. G.: Interacting effects of leaf water potential and biomass on vegetation optical depth, J. Geophys. Res. Biogeosci., 122, 3031–3046, https://doi.org/10.1002/2017JG004145, 2017.

Myneni, R. B., Hall, F. G., Sellers, P. J., and Marshak, A. L.: The interpretation of spectral vegetation indexes, IEEE Trans. Geosci. Remote Sens., 33, 481–486, https://doi.org/10.1109/36.377948, 1995.

Piao, S., Wang, X., Park, T., Chen, C., Lian, X., He, Y., Bjerke, J. W., Chen, A., Ciais, P., Tømmervik, H., Nemani, R. R., and Myneni, R. B.: Characteristics, drivers and feedbacks of global greening, Nat. Rev. Earth Environ., 1, 14–27, https://doi.org/10.1038/s43017-019-0001-x, 2020.

Rao, K., Anderegg, W. R. L., Sala, A., Martínez-Vilalta, J., and Konings, A. G.: Satellite-based vegetation optical depth as an indicator of drought-driven tree mortality, Remote Sens. Environ., 227, 125–136, https://doi.org/10.1016/j.rse.2019.04.001, 2019.

Sen, P. K.: Estimates of the regression coefficient based on Kendall's tau, J. Am. Stat. Assoc., 63, 1379–1389, https://doi.org/10.2307/2285891, 1968.

Tian, F., Brandt, M., Liu, Y. Y., Verger, A., Tagesson, T., Diouf, A. A., Rasmussen, K., Mbow, C., Wang, Y., and Fensholt, R.: Remote sensing of vegetation dynamics in drylands: Evaluating vegetation optical depth (VOD) using AVHRR NDVI and

https://doi.org/10.5194/egusphere-2026-3311
Preprint. Discussion started: 30 June 2026

in situ green biomass data over West African Sahel, Remote Sens. Environ., 177, 265–276, https://doi.org/10.1016/j.rse.2016.02.056, 2016.

Tian, J., Luo, X., Fang, Y., Zhu, C., Su, H., Ding, J., Li, G., and Peng, B.: Conflicting changes of vegetation greenness interannual variability on half of the global vegetated surface, Earth's Future, 12, e2023EF004119, https://doi.org/10.1029/2023EF004119, 2024.

Zhu, Z., Piao, S., Myneni, R. B., Huang, M., Zeng, Z., Canadell, J. G., Ciais, P., Sitch, S., Friedlingstein, P., Arneth, A., Cao, C., Cheng, L., Kato, E., Koven, C., Li, Y., Lian, X., Liu, Y., Liu, R., Mao, J., Pan, Y., Peng, S., Peñuelas, J., Poulter, B., Pugh, T. A. M., Stocker, B. D., Viovy, N., Wang, X., Wang, Y., Xiao, Z., Yang, H., Zaehle, S., and Zeng, N.: Greening of the Earth and its drivers, Nat. Clim. Change, 6, 791–795, https://doi.org/10.1038/nclimate3004, 2016.

Zotta, R.-M., Moesinger, L., van der Schalie, R., Vreugdenhil, M., Preimesberger, W., Frederikse, T., de Jeu, R., and Dorigo, W.: VODCA v2: multi-sensor, multi-frequency vegetation optical depth data for long-term canopy dynamics and biomass monitoring, Earth Syst. Sci. Data, 16, 4573–4617, https://doi.org/10.5194/essd-16-4573-2024, 2024.